

Coupling between Neuronal Firing Rate, Gamma LFP, and BOLD fMRI Is Related to Interneuronal Correlations

Yuval Nir,¹ Lior Fisch,¹ Roy Mukamel,²
Hagar Gelbard-Sagiv,¹ Amos Arieli,¹ Itzhak Fried,^{3,4}
and Rafael Malach^{1,*}

¹Department of Neurobiology
Weizmann Institute of Science
Rehovot 76100
Israel

²Ahmanson Lovelace Brain Mapping Center
Neuropsychiatric Institute
David Geffen School of Medicine
University of California, Los Angeles
Los Angeles, California 90095

³Division of Neurosurgery
David Geffen School of Medicine and Semel Institute
for Neuroscience and Human Behavior
University of California, Los Angeles
Los Angeles, California 90095

⁴Functional Neurosurgery Unit
Tel Aviv Medical Center and Sackler School of Medicine
Tel Aviv University
Tel Aviv 69978
Israel

Summary

Background: To what extent is activity of individual neurons coupled to the local field potential (LFP) and to blood-oxygenation-level dependent (BOLD) functional magnetic resonance imaging (fMRI)? This issue is of high significance for understanding brain function and for relating animal studies to fMRI, yet it is still under debate.

Results: Here we report data from simultaneous recordings of isolated unit activity and LFP by using multiple electrodes in the human auditory cortex. We found a wide range of coupling levels between the activity of individual neurons and gamma LFP. However, this large variability could be predominantly explained ($r = 0.66$) by the degree of firing-rate correlations between neighboring neurons. Importantly, this phenomenon occurred during both sensory stimulation and spontaneous activity. Concerning the coupling of neuronal activity to BOLD fMRI, we found that gamma LFP was well coupled to BOLD measured across different individuals ($r = 0.62$). By contrast, the coupling of single units to BOLD was highly variable and, again, tightly related to interneuronal-firing-rate correlations ($r = 0.70$).

Conclusions: Our results offer a resolution to a central controversy regarding the coupling between neurons, LFP, and BOLD signals by demonstrating, for the first time, that the coupling of single units to the other measures is variable yet it is tightly related to the degree of interneuronal correlations in the human auditory cortex.

Introduction

Understanding brain function through analysis of experimental data requires an understanding of the types of neuronal activities that are manifested in the recorded signals and of how to relate different measures to each other. With the exponential growth in functional magnetic resonance imaging (fMRI) research, an important challenge is to try and bridge the gap between noninvasive human studies examining changes in the blood-oxygenation-level dependent (BOLD) fMRI signal and the extensive body of research obtained through electrophysiological recordings in animals, typically examining the spiking activity of individual neurons. Central to this issue is the following question: Under what circumstances are spiking activity of individual neurons, high-frequency (gamma) local field potential (LFP), and BOLD fMRI well correlated with one another?

Although the biophysical origin of spiking activity is well understood [1], less is known about the origin of LFPs. Simultaneous studies of spiking activity and LFPs, combined with current source-density analysis, suggest that the LFPs arise from the combined activity of large numbers of neurons distributed over a large region of the cortex [2]. LFPs are believed to primarily arise from dendritic activity and thus provide a measure of the input to, and local processing within, an area [2, 3]. Several recent studies have also pointed to the role of power changes in the high-gamma band LFP (above 40 Hz) in sensory processing [4–6].

In addition, a growing number of recent studies have pointed to the possibility of a tight correlation between the BOLD signal and gamma LFP [7–9]. However, the relationship of neuronal spiking activity to both gamma LFP and the BOLD signal remains controversial. For instance, in studies that directly compared gamma LFP, single-unit activity, and BOLD in area V1 of anesthetized monkeys, it was found that compared to the gamma power, single-unit activity was less correlated with BOLD activity. This has led to the suggestion that these two measures can be uncoupled, particularly during extended stimulus durations [7, 8, 10]. Similarly, on the basis of optical recordings in anesthetized cats, Niessing and colleagues have shown that single units were decoupled from gamma power and from the BOLD-related optical signal when stimulation conditions were constant [11]. Similar dissociations between spiking activity and gamma LFP have been found in the cerebellar cortex of anesthetized rats [12], as well as in the visual cortex of cats [13] (for review, see [14]). The prevailing interpretation proposes that such dissociations stem from the fact that gamma power and BOLD fMRI represent summed synaptic currents [2], whereas single-unit spiking activity represents local outputs.

On the other hand, other studies have argued for a tight linear coupling between spiking activity and BOLD responses. Two theoretical studies have suggested that a high correlation exists between fMRI BOLD changes

*Correspondence: rafi.malach@weizmann.ac.il

in humans and spike recordings obtained under comparable experimental conditions in macaque monkeys [15, 16]. Such a linear relationship was also demonstrated empirically with simultaneous recordings in the anesthetized rat [17, 18] and for negative BOLD responses in anesthetized monkeys [8]. Recently, comparing spiking activity, gamma LFP, and BOLD signals obtained from human auditory cortex during natural stimulation conditions, we have shown a surprisingly high correlation between the spiking activity of a local neuronal population, gamma LFP, and the BOLD signal, despite the fact that these measures were obtained from different individuals [9]. It thus appears that the relationships between spiking activity, gamma LFP, and BOLD are quite inconsistent and change markedly from one experimental preparation to another.

In our earlier study [9] we have assumed a constant level of coupling between the averaged spiking activity of a neuronal population, gamma LFP, and BOLD. In the present study, we extended our examination and explored how the coupling of individual neurons to gamma LFP and BOLD changed over time and whether we could identify parameters that may correlate to these changes. We found that gamma LFP exhibited a sustained level of strong coupling to the BOLD signal. By contrast, the level of correlation between the activity of each individual neuron and the gamma LFP or the BOLD signals varied substantially over time. These changes were strongly related to the level of correlation in firing rates among neighboring neurons. Importantly, this relation was not due solely to the stimulus properties because it persisted also during spontaneous activity. It should be emphasized that the firing-rate modulations we refer to were relatively slow (>80 ms) and are not relevant to the issue of precise spike synchrony (on time scales of <10 ms). The present study focused on the slow modulations in firing rates and gamma power changes because these have been found to be correlated to BOLD fMRI [7, 9, 11].

Thus, our data suggest that the coupling between the activity of individual neurons and gamma LFP as well as BOLD is correlated with the extent to which the activity of these individual neurons corresponds to the overall firing rate within the local neuronal population. To the best of our knowledge, this is the first time that a relationship between multiple isolated units and gamma LFP power changes has been demonstrated in the awake, behaving primate. Since recent studies indicate that hemodynamic coupling to neural activity can be strongly modulated by anesthesia [19], our results are particularly relevant to the question of what neural activity underlies fMRI measurements in the alert human brain.

Results

Wide Range of Spike-Gamma Coupling Levels

Our study consisted of 59 neurons recorded from three human subjects. Electrode locations were in the bilateral auditory cortex, as determined by coregistration of CT scans after electrode implantation with preoperative MRI. Table S1 (in the Supplemental Data available online) provides the details of the recordings. Our experimental paradigm consisted of two main conditions: a 9 min segment of a popular audio-visual movie, which was repeated twice, and a 5–10 min rest period, in which

no stimuli were presented. In the remainder of the paper we will refer to the activity in the absence of stimulation as “spontaneous” activity (see Supplemental Experimental Procedures for additional details). Well-isolated neurons (see Supplemental Experimental Procedures for criteria of isolation) were considered responsive to the movie on the basis of reproducibility of responses across the two presentations, and 59 out of 75 units were then selected for further analysis.

The stimulus selectivity of the neuronal responses to the naturalistic stimuli was typically rather specialized and complex, showing both broad and extremely narrow frequency selectivity under different stimulus conditions. However, a fully detailed description of these highly complex auditory properties is beyond the scope of this manuscript and will be treated extensively elsewhere (Y. Bitterman, personal communication).

Figure 1 shows two examples of spike trains from one isolated neuron and simultaneously recorded LFP from the same microelectrode during different segments of the movie presentation. As can be seen, during some time segments, the movie elicited highly modulated spike trains (Figure 1A), which exhibited a strong correlation with gamma-power modulations of the simultaneously acquired LFP ($r = 0.84$). However, during other segments (Figure 1B), the correlation of the same neuron with gamma-power modulations of the LFP was substantially weaker ($r = 0.19$). We therefore set out to examine this variability in detail.

We first characterized the LFP by examining its typical spectral content. As others have recently demonstrated [5, 20], the power in the LFP spectra dropped with increasing frequency and could roughly be approximated as “ $1/f^2$ ” (where f is the frequency) (Figure S1). However, unlike some previous studies [5, 20, 21], we did not find a sharply localized peak around 40 Hz, and our use of the term “gamma-band” refers therefore to the broad range of frequencies (40–130 Hz) that have been reported to be highly correlated to fMRI BOLD signals [7, 9] (see also Discussion). In our treatment of the LFP signals, we concentrated on band-limited power (BLP) modulations [7, 9] (see also Supplemental Experimental Procedures). In the remainder of this paper, unless explicitly indicated, we will refer to the correlations between gamma BLP modulations and single-unit-firing-rate modulations as the spike-gamma coupling.

Next, we divided the movie timeline into 10 s long segments (see Supplemental Experimental Procedures for more details) and examined the spike-gamma coupling level in each segment separately. Note that this coupling level captures the similarity between instantaneous modulations in firing rates and instantaneous modulations in gamma power throughout the segment, as shown in Figure 1. This examination revealed a wide range of coupling levels (correlations) during movie stimulation (Figure 2A, mean = 0.30, SD = 0.22). A wide range of coupling levels was also found during spontaneous activity, albeit with a lower mean coupling level (mean = 0.19, SD = 0.18). In addition, because of the spatial extent of the LFP signals, we also found a significant spike-gamma coupling between spiking activity recorded in one microelectrode and gamma LFP on different electrodes (Figure S2). In order to aid visualization in the following figures, we divided the data into five subsets,

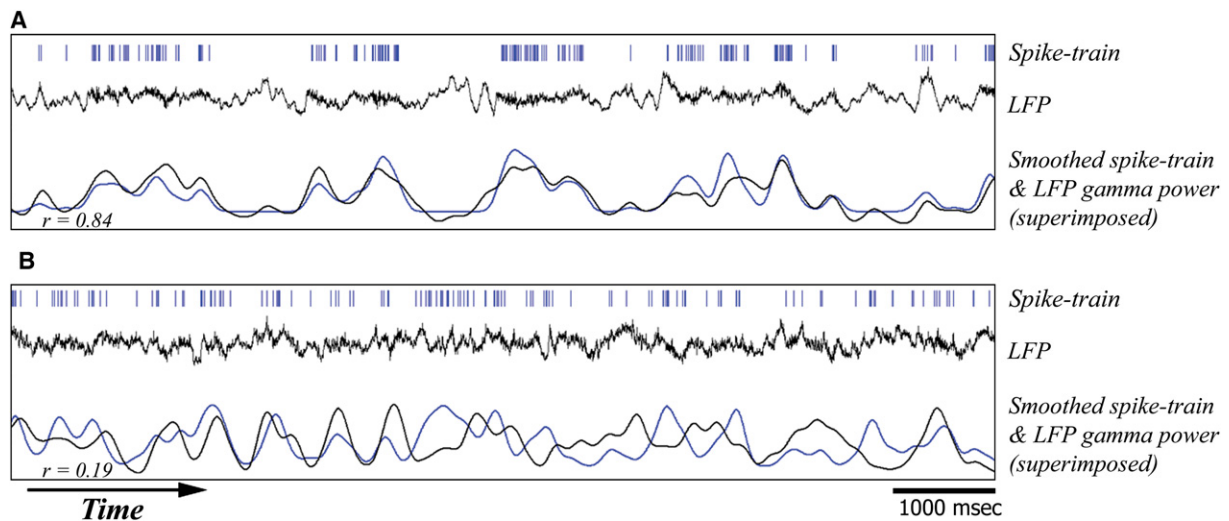


Figure 1. Example Spike Trains and LFPs

Data from one isolated neuron (mean firing rate = 14 Hz) and the simultaneously recorded LFP from the same microelectrode during segments of movie stimulation associated with strong or poor coupling of spikes to gamma LFP.

(A) Strong coupling: Data acquired during a 10 s segment associated with strong spike-gamma coupling ($r = 0.84$). Rows (top to bottom) correspond to: (1) spike train, (2) raw LFP filtered below 130 Hz, and (3) smoothed spike train and gamma-band power modulations superimposed; each time-course value represents the instantaneous firing rate (blue) or gamma power (black) at that time.

(B) Poor coupling: Data from the same neuron and microelectrode acquired during a different 10 s segment associated with poor spike-gamma coupling ($r = 0.19$). Rows and colors are as shown in (A). Note that in this data segment, changes in firing rate are poorly correlated to changes in LFP gamma power (bottom row).

according to the magnitude of correlation between gamma LFP and spiking activity. Examining these different subsets for the correlations of spiking activity with power changes in various LFP frequency bands (Figure 2B) revealed that segments with strong spike-gamma coupling ($r = 0.6$, red trace) were associated with a mild anticorrelation between spiking activity and low-frequency LFP ($r = -0.17$, red trace). This may be related to the fact that segments with strong spike-gamma coupling were associated with less power in low-frequency LFP, such as the alpha band (8–14Hz) (Figure S3).

We also found that the time course of spike-gamma coupling changes was reproducible across the two movie presentations ($r = 0.33$, $p < 0.001$). Figure 3 shows the mean changes in spike-gamma coupling during the movie, averaged across all 59 neurons and superimposed on the basic sound-wave amplitude, as well as high-order auditory events such as the occurrence of speech and musical phrases. High levels of spike-gamma coupling were poorly correlated to sound-wave amplitude ($r = -0.14$, $p = 0.32$) but strongly related to the occurrences of speech ($r = 0.45$, $p < 0.001$). This clearly indicates that during movie stimulation, changes in spike-gamma coupling levels were related to a specific aspect of the stimulus and could not be explained by random dynamic changes in noise sources.

The wide range of coupling levels we observed replicates the entire spectrum of recently published findings regarding the relationship between single-unit activity and gamma LFP, ranging from strong coupling (red line, Figure 2B) to considerable decoupling (yellow lines, Figure 2B). Importantly, because we reproduced this diversity in the same subjects and experimental preparation, we could now search for parameters that may be related to this diversity.

Spike-Gamma Coupling Is Related to Correlations between Neurons

We found that the main parameter that covaried with spike-gamma coupling levels was the degree of correlation between adjacent neurons. At first, we compared the level of correlation between the spiking activities of neighboring neurons during segments associated with strong versus poor spike-gamma coupling. This comparison was assessed quantitatively by calculating the spike cross-correlation function between simultaneously recorded neighboring neurons [22]. Figure 4A depicts the results of this analysis as applied on unsmoothed binary spike trains. As can be seen, correlations between neighboring neurons were more pronounced and prolonged during segments of strong spike-gamma coupling (red trace) than during segments of poor spike-gamma coupling (yellow trace). Note that such correlations reflect comodulation of firing rates lasting up to hundreds of milliseconds and do not necessarily reflect precise co-occurrence of action potentials. In the remainder of the paper, we use the term “correlations between neurons” to refer to such, relatively slow, firing rate correlations. It is important to clarify that the term “correlations between neurons” in this paper does not differentiate between correlations driven by common sensory inputs and other sources (“noise correlations”).

Next, we examined whether the changes in the correlations between neurons could be related to the variability observed in the spike-gamma coupling over time. To that end, we performed the following analysis: By using a sliding window, we calculated the time course of the averaged correlations between neurons during the movie (Figure 4B, green trace). We then superimposed on this graph the time course of spike-gamma coupling

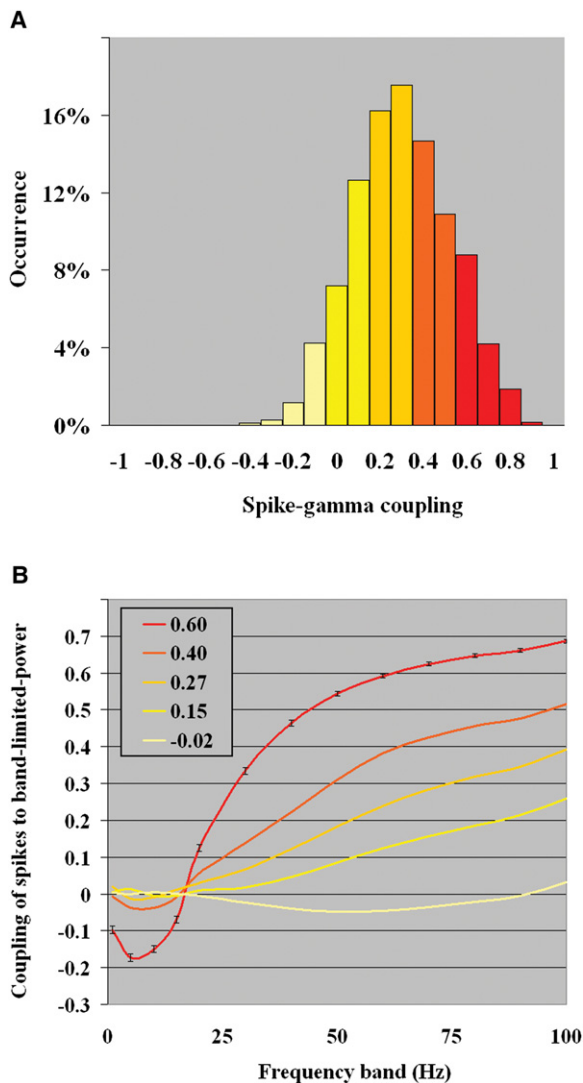


Figure 2. Spike-Gamma Coupling Levels
(A) Distribution of spike-gamma coupling levels during movie stimulation: The distribution of correlation coefficients between firing-rate modulations of individual neurons and gamma-band (40–130 Hz) power modulations. Yellow to red colors illustrate the division of data segments into five equal grades on the basis of these correlations. $n = 2315$ segments. Mean coupling level = 0.3; SD = 0.22.
(B) Spike-LFP coupling as a function of frequency band: Correlation between firing rates of individual neurons and band-limited power (BLP) in various frequency bands as a function of the frequency band of interest. Each line denotes the mean result for all 10 s segments associated with a specific coupling level to the gamma BLP. Yellow to red colors indicate increasing levels of spike-gamma coupling in the movie data as shown in (A). Error bars indicate SEM between separate data segments. $n = 463$ segments for each grade.

during the movie (Figure 4B, red trace). As can be seen, the degree of correlations between neighboring neurons and the degree of spike-gamma coupling showed a strong level of covariation ($r = 0.91$, $p < 0.001$).

A quantitative analysis of the entire movie data set, divided into nonoverlapping segments (Figure 4C), revealed that the level of correlations between neurons was strongly related to the levels of spike-gamma coupling ($r = 0.66$, $p < 0.001$). This result establishes that a large part of the variability in spike-gamma coupling

levels during stimulation can be explained by interneuronal correlations.

Moreover, we found that the relation between interneuronal correlations and spike-gamma coupling was not a purely stimulus-driven phenomenon, because a similar analysis performed on the spontaneous data set (Figure 4D) revealed that the level of correlations between neurons was related to the levels of spike-gamma coupling even when external sensory input was predominantly absent ($r = 0.48$, $p < 0.001$). This result indicates that a significant part, but not all, of the variance in spike-gamma coupling and interneuronal correlations may be derived from intrinsic sources within the brain. These phenomena could not be attributed to between-subjects or between-sessions effects because they could also be found within single sessions (Table S2).

Finally, we used a nonparametric bootstrapping procedure (Figure S4) to compare the correlation coefficients found during stimulation ($r = 0.66$ as shown in Figure 4C) and spontaneous activity ($r = 0.48$ as shown in Figure 4D). The difference between the correlation coefficients was found to be statistically significant ($p < 0.001$, Figure S4), indicating that both intrinsic and extrinsic sources have a significant contribution to the relation between spike-gamma coupling and interneuronal correlations (see also Discussion).

Spike-Gamma Coupling Cannot Be Explained by Changes in Firing Rates

It may be argued that the enhanced spike-gamma coupling, as well as the increased correlation between neighboring neurons, was simply a consequence of better signal-to-noise conditions that occurred whenever there were higher firing rates. Segments of strong spike-gamma coupling were indeed associated with higher firing rates ($r = 0.47$, Figure S3). In order to examine this possibility, we selected segments that are associated with either low or high levels of correlations between different neurons, but that have equal average firing rates, and compared the spike-gamma coupling levels during these segments. The results are shown in Figure 5 and clearly demonstrate that even under equal average firing rates and signal-to-noise measures, the correlations between neighboring neurons were strongly related to the degrees of spike-gamma coupling.

In addition, we conducted a three-way, repeated-measures ANOVA with firing rate (representing spike SNR), gamma power (representing LFP SNR), and correlations between neurons as factors. This analysis revealed that a significant part of the variability in spike-gamma coupling could be attributed to changes in correlations between neurons, beyond the contributions of signal-to-noise ratios of spiking activity and LFP ($F_{2,315} = 541$, $p < 0.001$).

Spike-BOLD Coupling Is Also Related to Correlations between Neurons

Recently, we reported a strong coupling between the spiking activity of a local neuronal population, gamma LFP, and fMRI BOLD signals by using the same paradigm [9]. It was thus of interest to extend the analysis to the correlation between individual neurons' spiking activity and the BOLD signals. It should be noted that in our experimental setup, the BOLD responses were

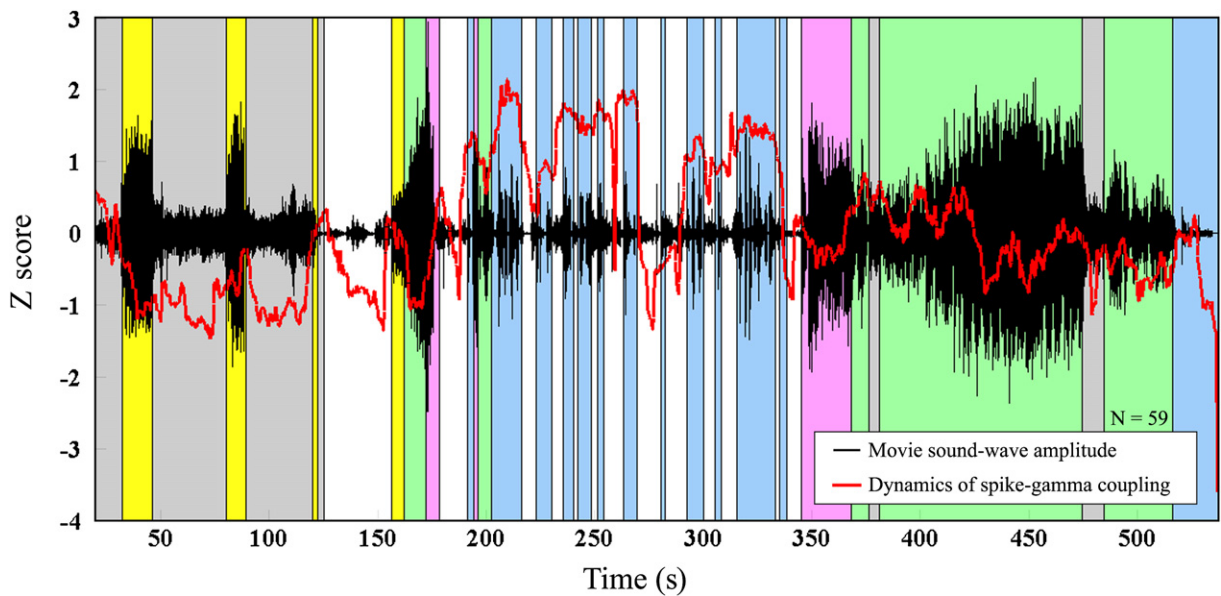


Figure 3. Relating Spike-Gamma Coupling to Auditory Stimulus

The mean dynamics of spike-gamma coupling (red) during the movie presentations, averaged across 59 neurons, are plotted against the auditory sound-wave amplitude (black) and the category of auditory events as follows: gray, background noises; yellow, horses and people marching; white, quiet; green, music; pink, gunshots and explosions; and blue, speech and dialog. Note that high spike-gamma coupling is related to the occurrence of speech utterances ($r = 0.45$, $p < 0.001$).

not recorded in the same individuals as the neuronal activity. Consequently, for comparison between the two data sets, it was critical to use only segments in which all subjects displayed similar auditory responses. We therefore selected for analysis only those segments where there was a high intersubject correlation in the fMRI responses to the movie [9, 23] (see also [Supplemental Experimental Procedures](#)).

In order to compare the electrical signals to changes in BOLD fMRI, we first convolved both the changes in LFP gamma power (gamma BLP) and the spike trains of each neuron with a hemodynamic impulse response function (see [Supplemental Experimental Procedures](#)). Next, by using a sliding window, we calculated the time course of gamma-BOLD coupling levels (Figure 6A, yellow trace). As can be seen, despite the across-subject variation, the gamma-BOLD coupling was particularly strong and relatively constant during this session ($r = 0.8$, $p < 0.001$). We then superimposed on this graph the time course of spike-BOLD coupling during the movie (Figure 6A, blue trace). We found that in contrast to the gamma-BOLD coupling, the coupling of individual neurons to fMRI BOLD was highly variable. However, superimposing the time course of correlations between neurons (Figure 6A, green trace) revealed that there was a strong relationship between the degree of correlations among neighboring neurons and the degree of spike-BOLD coupling in this recording session ($r = 0.82$, $p < 0.001$).

We then conducted a quantitative analysis on the entire data set, divided into nonoverlapping segments (Figures 6B and 6C), computed the single-unit-to-BOLD and gamma-BOLD correlations for each segment, and compared them to the level of correlations between neurons. This analysis confirmed that gamma LFP was more strongly coupled to fMRI BOLD than was spiking activity of individual neurons ($r = 0.62$ for gamma versus

$r = 0.47$ for spikes, $p < 0.001$, paired t test). In addition, we found that the level of correlation between neurons could serve as a good predictor for the level of spike-BOLD coupling ($r = 0.70$, $p < 0.001$) but could only serve as a poor predictor for the level of gamma-BOLD coupling ($r = 0.26$, $p < 0.001$), which exhibited less variability and remained constantly at a high level ($p < 0.001$, F test for equal variance). Finally, these phenomena could not be attributed to between-subjects or between-sessions effects because they could also be found in single sessions (Table S2).

We performed an additional control by repeating this analysis with a BOLD signal sampled from the primary visual cortex. This analysis revealed that spiking activity in the auditory cortex was not significantly correlated with visual cortex BOLD ($r = 0.03$, $p = 0.40$), nor were correlations between neurons in auditory cortex predictive of the spike-BOLD coupling in this case ($r = 0.04$, $p = 0.13$). Similar results were obtained for gamma LFP from auditory cortex: It was not correlated with visual cortex BOLD ($r = 0.05$, $p = 0.38$), nor were correlations between neurons in auditory cortex predictive of the LFP-BOLD coupling in this case ($r = 0.02$, $p = 0.28$).

In summary, we found a wide range of spike-gamma coupling levels when measuring the responses of individual neurons. The level of this coupling was tightly linked to the degree of correlation between neighboring neurons, both during movie stimulation and during spontaneous activity. When extending our analysis to BOLD fMRI, we found that the gamma-BOLD coupling was strong and relatively stable despite the fact that it was measured across individuals. By contrast, the coupling of single-unit activity to BOLD varied substantially and, as in the case of the spike-gamma coupling, was also tightly correlated with the degree of coactivation among neighboring neurons.

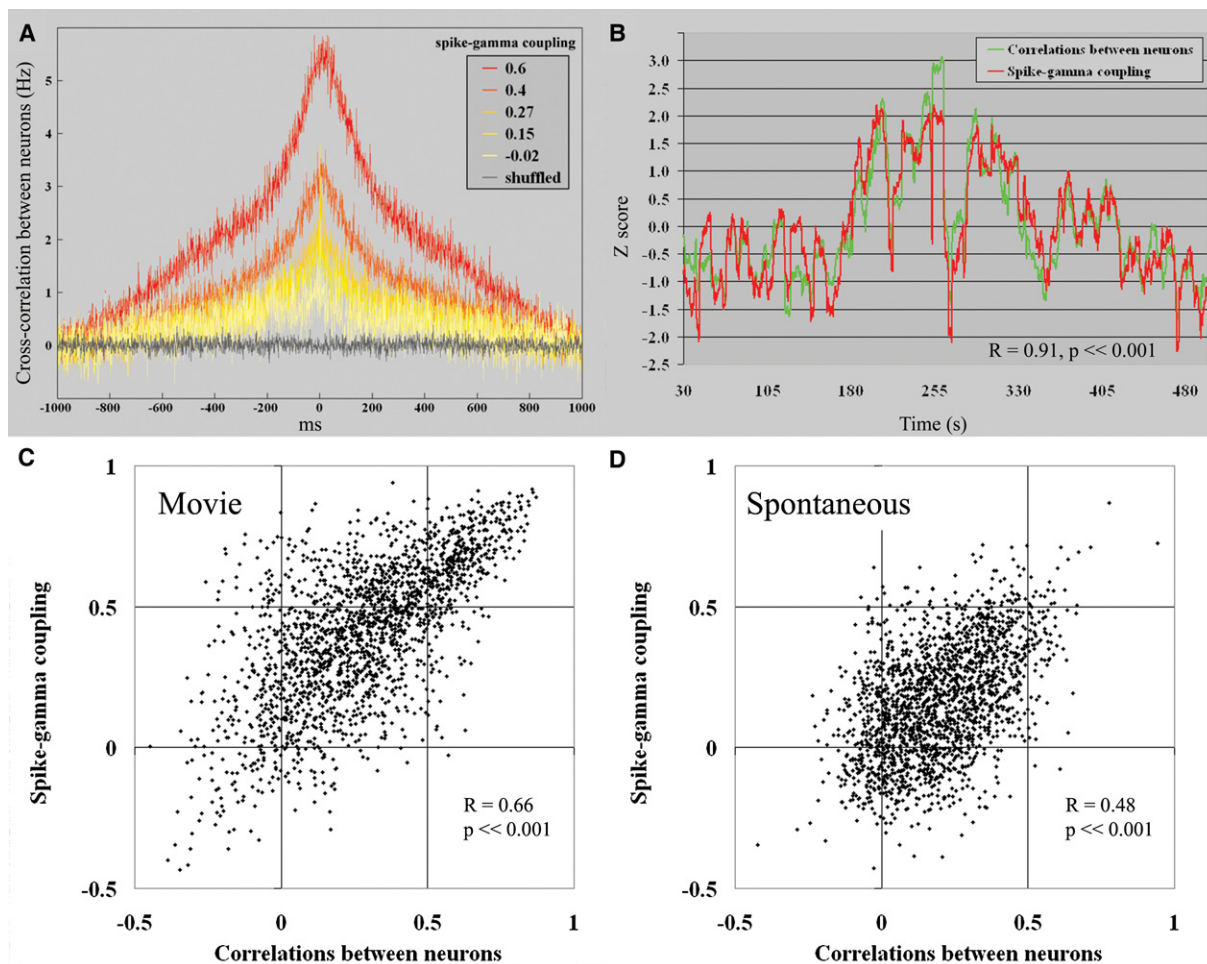


Figure 4. Spike-Gamma Coupling Is Related to Correlations between Neighboring Neurons

(A) Normalized spike cross-correlation between neighboring neurons (correlations between binary spike trains of different neurons at millisecond resolution) for each degree of spike-gamma coupling. Gray indicates the control (shuffled data); yellow to red colors indicate increasing levels of spike-gamma coupling in the movie data (see legend). $t = 0$ indicates the occurrence of the triggering spikes. Note that strong spike-gamma coupling (red) is associated with increased cross-correlations between neurons over prolonged (hundreds of milliseconds) periods of time. $n = 59$ neurons, 171 pairs of neurons.

(B) Time courses of spike-gamma coupling and correlations between neurons in one recording session. The time course of spike-gamma coupling in one movie-stimulation session ($n = 10$ neurons) superimposed with the time course of correlations between neurons (mean of pairwise correlations) during that session; each value represents the level of spike-gamma coupling (red) or the level of correlations between neurons (green) in a data segment around that time. Note the tight correspondence between the waxing and waning of the two phenomena over time ($r = 0.91$, $p << 0.001$).

(C) Spike-gamma coupling versus correlations between neurons—movie-stimulation data: A scatter plot of the level of spike-gamma coupling versus the level of correlations between neurons for all sensory stimulation data segments is shown ($n = 2315$ data segments/dots, based on data of 59 neurons, $r = 0.66$, $p << 0.001$). Each dot in the scatter reflects one segment of data of a particular neuron, for which we computed the two following measures: (1) the degree of spike-gamma coupling for that neuron at that time (y axis) and (2) the degree of correlation between the activities of that neuron to the activities of all neighboring neurons (mean pairwise correlations, x axis).

(D) Spike-gamma coupling versus correlations between neurons—spontaneous (no stimulus) data: A scatter plot of the level of spike-gamma coupling versus the level of correlations between neurons for all no-stimulus data segments is shown ($n = 2315$ data segments/dots, based on data of 59 neurons, $r = 0.48$, $p << 0.001$). Each dot in the scatter reflects one segment of data of a particular neuron, as explained above. Note that although the mean levels of spike-gamma coupling and correlations between neurons are lower in the absence of stimulation, the tight correspondence between the two phenomena persists.

Discussion

Diversity in Coupling between Individual Neurons, Gamma LFP, and BOLD

The variable nature of the spike-gamma correlation has been a source of intensive debate and concern, both in terms of understanding brain function [6] and because of its significance to fMRI research [10]. The diversity of spike-gamma coupling levels reported in different

studies (see Introduction) may be explained by a number of factors such as species, anesthesia, sensory stimuli, behavioral task, and brain regions. However, here we have demonstrated that in the auditory cortex of conscious humans, such diversity may occur within the same recording session (Figure 2A). The time course of spike-gamma coupling changes was reproducible across repeated presentations of the movie and therefore could not be attributed to changes in noise source

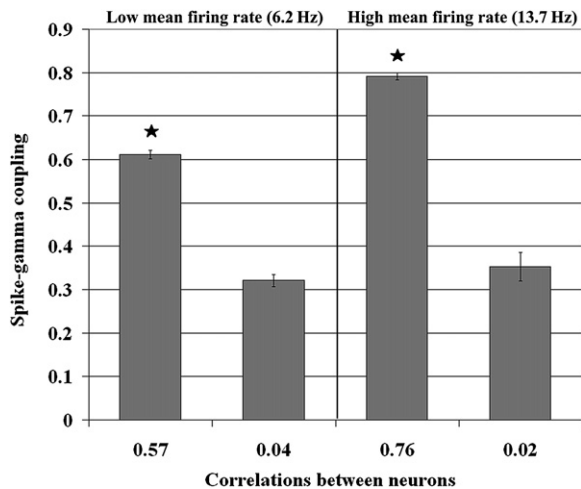


Figure 5. Spike-Gamma Coupling Cannot Be Explained Simply by Changes in Firing Rates

Spike-gamma coupling in data segments with equal mean firing rates but different levels of correlations between neurons. Left and right pairs of bars denote data segments with the same low (6.2 Hz) or high (13.7 Hz) mean firing rates but with different levels of correlations between neurons (shown below the histograms). All bars include data from the same neurons. Error bars indicate SEM between separate data segments. Note that spike-gamma coupling is strongly related to the degree of correlations between neurons even when mean firing rates (and signal to noise) are equal (stars indicate $p < 0.001$, paired t test, $n = 310$ data segments per category).

such as movement or recording issues. In fact, high levels of spike-gamma coupling were related to the occurrence of speech utterances during movie presentation (Figure 3), indicating that during stimulation, the changes in spike-gamma coupling levels were predominantly stimulus driven. On the other hand, a similar diversity could be found also during spontaneous activity in the absence of sensory stimulation, indicating that changes in spike-gamma coupling could not be attributed only to stimulus-driven common inputs.

Spike-Gamma Coupling Is Related to Correlations between Neurons

Our ability to record simultaneously from several well-isolated neurons allowed us to relate the variability in spike-gamma coupling to other neuronal phenomena. Here we show that the changes in spike-gamma coupling can be largely predicted by measuring the level of correlations in firing rates between neighboring neurons (Figure 4). Simply put, whenever the firing rate of a single recorded neuron appeared to correspond to the overall activity of a distributed neuronal population, the spike-gamma correlations were high, and whenever each neuron manifested independent activation from its neighbors, the spike-gamma correlations were low. An analogous phenomenon has been recently reported in the monkey IT cortex [24]. However, to the best of our knowledge, this is the first demonstration of a correlation between single-unit comodulation and gamma power changes.

It is often suggested that the breakdown of spike-gamma coupling is due to a fundamental dissociation of synaptic inputs from the spiking output [10]. However, the current observations point to another explanation

that is not necessarily mutually exclusive with the former: the dissociation of the activity of individual neurons from that of their local population. Thus, in studies that reported low spike-gamma coupling during sustained stimulation (e.g., [11]), at least some contribution to this low coupling may have been due to uncorrelated activity among individual neurons.

What are the factors contributing to the relationship between correlated firing and gamma power? One possibility is that these two measures were related because of extrinsic factors, i.e., a strong stimulus-driven input that produced simultaneous activation and enhanced gamma power leading to the observed spike-gamma coupling. However, we also found a strong association between these phenomena during spontaneous activity, in the absence of external stimuli, indicating that intrinsic factors within the brain also contribute to this relationship. Comparing the statistical significance of the spontaneous and movie-driven effects through a bootstrapping procedure revealed a tighter relation between the phenomena during movie stimulation than during spontaneous activity (Figure S4). This difference could possibly be due to a wider modulation range of the neuronal activity during movie stimulation as compared to spontaneous activity. Accordingly, the movie-stimulation data were associated with unique instances of particularly high positively and negatively correlated neurons (e.g., compare upper right and lower left quadrants in Figures 4C and 4D).

What are the neuronal mechanisms underlying the relationship between correlated firing and gamma power? It has been suggested that population activity is related to gamma-band energy through inhibitory neuronal signaling [21]. The current results are also compatible with a simpler model, in which the synaptic input expressed by the LFP is for the most part directly linked to the output firing rates within the neuronal population. Such activity may be mediated by the dense local connectivity that is typical of cortical neurons [25, 26]. This model is also supported by recent findings demonstrating that gamma LFP is highly correlated with multiunit activity [6]. Given the great significance attributed to gamma-band LFP in high-level models of perception [27, 28], the possibility that changes in gamma power may reflect local increases in population firing rates should be of interest.

In our analysis, we only found marked correspondence between envelopes of firing rates and gamma-power changes over time windows longer than 100 ms. This may be related to the fact that in our experimental paradigm (which consisted of movie stimulation and rest) the spectrum of the LFP did not reveal a localized peak of 40–50 Hz gamma oscillations (Figure S1). Such oscillations have been often reported in other systems to be phase-locked to spiking activity and have been implicated in various aspects of cognitive function [29–34] (for reviews, see [27, 28]). Precise phase-locking has typically been found between spiking activity and gamma LFP in moments of increased attention [32], so it is possible that future work focusing on particular moments of heightened attention might reveal a similar phenomenon in human data. It should also be noted that some studies suggest that precise gamma phase-locking may be species specific [35], stimulus dependent [36], or more

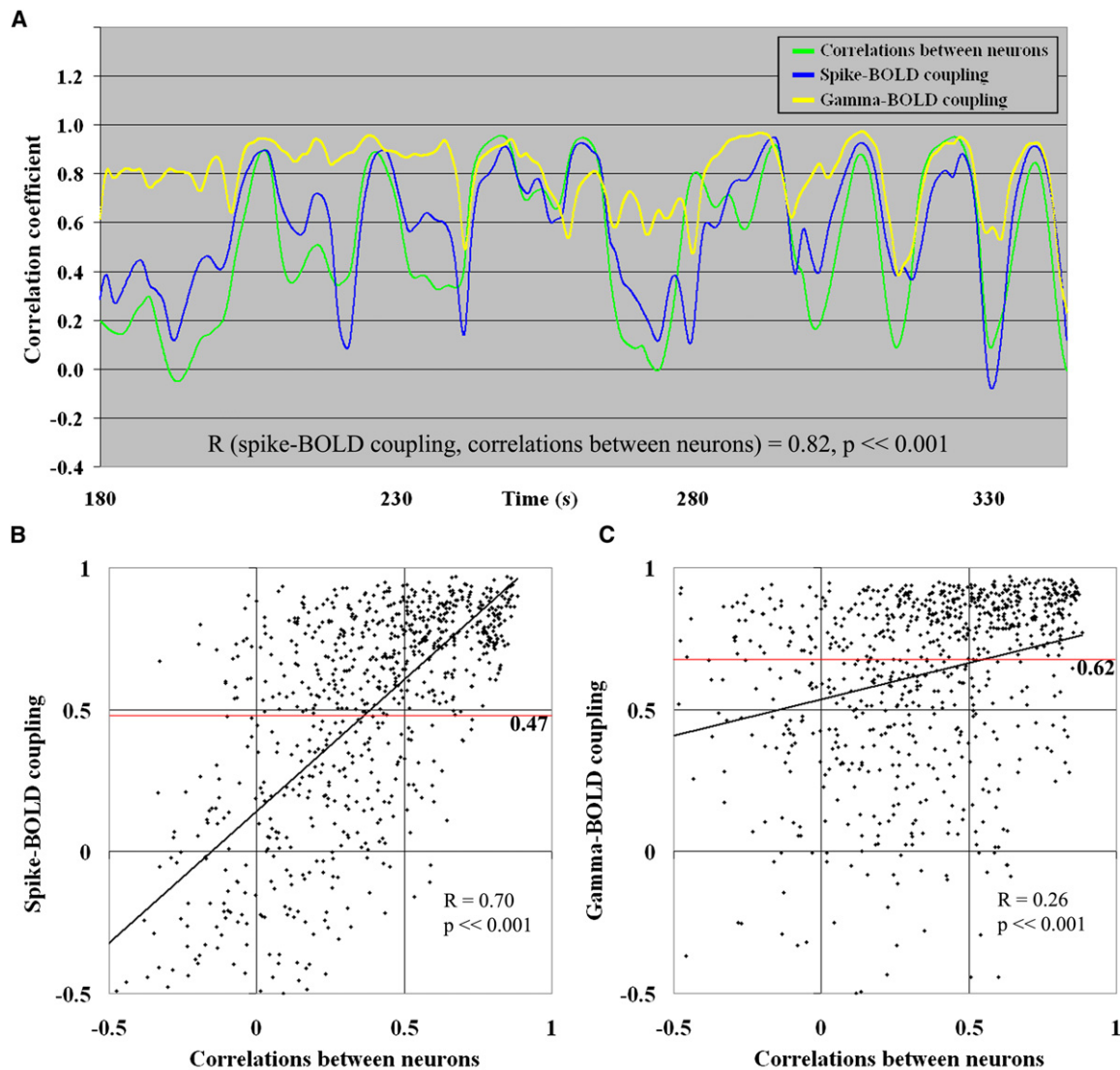


Figure 6. Spike-BOLD Coupling Is Related to Correlations between Neighboring Neurons

(A) Time courses of spike-BOLD coupling, gamma-BOLD coupling, and correlations between neurons in one recording session. The same spike trains and gamma-power changes used in Figure 4B ($n = 10$) were first convolved with a hemodynamic response function to allow comparison with fMRI BOLD signals (see Supplemental Experimental Procedures). We then compared the time courses of correlations between neurons, spike-BOLD coupling, and gamma-BOLD coupling. Each value represents the level of spike-BOLD coupling (blue), the level of gamma-BOLD coupling (yellow), or the level of correlations between neurons (green) in a data segment around that time. Note that despite the across-individual comparison, the gamma-BOLD coupling is extremely high and stable. By contrast, spike-BOLD coupling is highly variable and tightly related to the degree of correlations between neurons ($r = 0.82$, $p \ll 0.001$).

(B) Spike-BOLD coupling versus correlations between neurons: A scatter plot of the level of spike-BOLD coupling versus the level of correlations between neurons for all data segments associated with high BOLD intersubject correlations is shown (see Supplemental Experimental Procedures, $n = 1158$ data segments/dots, based on data of 59 neurons, $r = 0.70$, $p \ll 0.001$). The horizontal red line denotes the mean level of coupling between single-unit spiking activity and BOLD ($r = 0.47$).

(C) Gamma-BOLD coupling versus correlations between neurons: A scatter plot of the level of gamma-BOLD coupling versus the level of correlations between neurons for all data segments associated with high BOLD intersubject correlations is shown (see Supplemental Experimental Procedures, $n = 1158$ data segments/dots, based on data of 59 neurons, $r = 0.26$, $p \ll 0.001$). Note that gamma-BOLD correlations are less related to changes in correlations between neurons than are spike-BOLD correlations. The horizontal red line denotes the mean level of coupling between gamma power and BOLD ($r = 0.62$).

difficult to reveal in auditory cortex [37]. It should be noted that whereas narrow-band gamma oscillations around 40 Hz are likely to be related to inhibitory interneurons [5, 14, 21, 37–40], the strong correlations previously reported between gamma LFP and BOLD were associated with broad-band gamma effects (40–130 Hz) as we report here [7, 9, 11]. Such broad-band gamma

effects do not necessarily correspond to the same physiological process as the narrow peaking in gamma frequencies.

Spike-BOLD and Gamma-BOLD Coupling

Our fMRI results were obtained by comparing electrical signals recorded in some subjects to BOLD

measurements in other subjects under identical stimulation conditions. At first, this scheme might not seem like a valid and reliable methodology. Unquestionably, a failure to find strong correlations with such methodology could be attributed to intersubject variability, intersite variability within auditory cortex, etc. However, the fact that we found particularly high and constant levels of correlations between gamma LFP and BOLD (Figure 6) despite all intervening factors clearly demonstrates that our approach provides a reliable and valid means to examine the relation between these signals, even when simultaneous recordings in the human cortex are unavailable.

The present study supports the notion [9–11] that the BOLD signal is better correlated with gamma LFP than with individual neuron recordings: The coupling of gamma LFP to BOLD was constantly maintained at a high level and did not show modulations as substantial as those of the coupling between single units and BOLD (Figure 6).

The current findings are most relevant to the controversy regarding the relationship of the BOLD signal to firing rates of individual neurons. We demonstrate that this coupling was tightly related to the level of correlations between the recorded neurons (Figure 6). Thus, low coupling may not necessarily be due to a permanent dissociation between neuronal firing and BOLD but rather due to the fact that during certain moments, the neuronal firing, as measured in single neurons, represents uncorrelated neuronal activity. Accordingly, it may be that some of the failures to find high correlations between single neurons and BOLD may be attributed to our inability, during certain brain states, to extrapolate from the firing of a single neuron to the local population's spiking activity, which may be driving the BOLD signal in the imaged voxel. In our data (Figure 6), it appears that whenever neighboring neurons were highly correlated and thus a part of a distributed activity pattern, the correlation between the activities of each individual neuron and BOLD was also high.

However, it is also important to note that the present results are derived from conscious human cortex under a rather specific type of stimulus and behavior, so we can not fully extrapolate from these results to other stimuli and behavioral conditions, anesthetic levels, pharmacological treatments, or brain structures, in which the neuronal firing rate and BOLD may indeed be fundamentally decoupled [10, 12, 14]. However, at least for the coupling between gamma LFP and BOLD we have now obtained evidence for extensive correlations throughout the human visual cortex as well [41].

Spike-Gamma and Spike-BOLD Correlations as a Marker for Distributed Neuronal Representations

Although we have obtained our data by using multiple electrode recordings, the results suggest that changes in the level of slow interneuronal correlations could be detected simply by correlating each single neuron with the gamma LFP measured at the same recording electrode. Thus, to the extent that the current observations can be extrapolated to other species, sensory systems, stimuli, and behavioral tasks, we propose that by measuring the level of correlation between single-unit activities and gamma LFP or BOLD, one could predict

how distributed the activity profile is under these circumstances.

Intuitively, it seems that in order to assess the degree of correlation in an active population of neurons, one must record simultaneously from many neurons and use global measures of collective firing. However, recent studies have demonstrated that an examination of pairwise correlations between neurons can provide a good approximation of the collective behavior in the responses of many neurons [42]. The current study extends this interesting observation by suggesting that by using a single electrode, one can derive the level of correlated activity by comparing the activity of a single neuron to the population-related gamma LFP.

This study provides an important framework for predicting under what circumstances BOLD responses will be well coupled to single-unit responses by highlighting the relationship of correlated activity patterns to this coupling. Therefore, when a specific experimental paradigm is known to elicit distributed activity patterns in a given cortical region (e.g., responses of low-level auditory cortex to speech, or responses of low-level visual cortex to movies), the corresponding BOLD signal can be expected to be well coupled to the activity of individual neurons. On the other hand, our model predicts that in instances where neuronal activity is believed to be sparse (e.g., excitatory neuronal activity in the hippocampus [43]), gamma LFP and BOLD responses will appear to be less correlated to the dynamics of spiking activity in individual cells.

Because it is not entirely clear what conditions may create high correlations and what conditions create low correlations among neurons, and variability in interneuronal correlations can be found both during stimulus and rest conditions, we propose that the spike-gamma or spike-BOLD correlation can be regarded as a variable that, regardless of the stimulus conditions, may be used as an index for the level of correlated firing-rate modulations in the cortex: When individual neurons are poorly coupled to gamma LFP and BOLD, the neuronal activity probably reduces in size to small, neuronal ensembles. On the other hand, whenever individual neurons exhibit strong coupling to gamma LFP and BOLD, the underlying computation is probably highly distributed, involving large populations of comodulated neurons. Thus, our results suggest that gamma LFP and BOLD may reflect the overall local neuronal activity. However, it should be noted that the relationship between interneuronal correlations and such local neuronal activity may be rather complex and dependent on additional factors such as the topography of the local circuitry.

Conclusions

Our results reveal a wide range of coupling levels between the firing rates of individual neurons and gamma LFP power. The level of spike-gamma coupling was highly correlated to the degree of firing rate correlations between neighboring neurons. This phenomenon occurred during both sensory stimulation and spontaneous activity. In addition, we found that gamma LFP was well coupled to BOLD measured across different individuals. By contrast, the coupling of single units to BOLD was highly variable and, again, tightly related to interneuronal firing-rate correlations. Our results offer

a resolution to a central controversy regarding the coupling between neurons, LFP, and BOLD signals by suggesting that gamma LFP and BOLD signals are coupled to the correlated firing rate in a local population but not necessarily to the firing rate of single units, which may often be uncorrelated with the averaged behavior of the local population.

Supplemental Data

Experimental Procedures, six figures, and two tables are available at <http://www.current-biology.com/cgi/content/full/17/15/1275/DC1/>.

Acknowledgments

We thank the patients for their cooperation in participating in the study, M. Harel and R. Quiroga for help with spike clustering, A. D. Ekstrom, E. Isham, E. Ho, T. A. Fields, E. Behnke and C. Wilson for technical assistance, E. Vaadia for help with cross-correlation software, and David Heeger, Uri Hasson, and Robert Shapley for helpful discussions and feedback. This study was funded by Israel Science Foundation Center of Excellence, Benozyo Center for Neuronal Degeneration, Moskona Fund, and Dominique Center to R. Malach, US-Israel Binational Science Foundation grant to I. Fried and R. Malach, and a European Molecular Biology Organization long-term fellowship to R. Mukamel.

Received: March 14, 2007

Revised: June 24, 2007

Accepted: June 25, 2007

Published online: July 19, 2007

References

- Hodgkin, A.L., and Huxley, A.F. (1952). Propagation of electrical signals along giant nerve fibers. *Proc. R. Soc. Lond. B. Biol. Sci.* **140**, 177–183.
- Mitzdorf, U. (1985). Current source-density method and application in cat cerebral cortex: Investigation of evoked potentials and EEG phenomena. *Physiol. Rev.* **65**, 37–100.
- Logothetis, N.K. (2003). The underpinnings of the BOLD functional magnetic resonance imaging signal. *J. Neurosci.* **23**, 3963–3971.
- Siegel, M., and Konig, P. (2003). A functional gamma-band defined by stimulus-dependent synchronization in area 18 of awake behaving cats. *J. Neurosci.* **23**, 4251–4260.
- Henrie, J.A., and Shapley, R. (2005). LFP power spectra in V1 cortex: The graded effect of stimulus contrast. *J. Neurophysiol.* **94**, 479–490.
- Liu, J., and Newsome, W.T. (2006). Local field potential in cortical area MT: Stimulus tuning and behavioral correlations. *J. Neurosci.* **26**, 7779–7790.
- Logothetis, N.K., Pauls, J., Augath, M., Trinath, T., and Oeltermann, A. (2001). Neurophysiological investigation of the basis of the fMRI signal. *Nature* **412**, 150–157.
- Shmuel, A., Augath, M., Oeltermann, A., and Logothetis, N.K. (2006). Negative functional MRI response correlates with decreases in neuronal activity in monkey visual area V1. *Nat. Neurosci.* **9**, 569–577.
- Mukamel, R., Gelbard, H., Arieli, A., Hasson, U., Fried, I., and Malach, R. (2005). Coupling between neuronal firing, field potentials, and fMRI in human auditory cortex. *Science* **309**, 951–954.
- Logothetis, N.K., and Wandell, B.A. (2004). Interpreting the BOLD signal. *Annu. Rev. Physiol.* **66**, 735–769.
- Niessing, J., Ebisch, B., Schmidt, K.E., Niessing, M., Singer, W., and Galuske, R.A. (2005). Hemodynamic signals correlate tightly with synchronized gamma oscillations. *Science* **309**, 948–951.
- Mathiesen, C., Caesar, K., Akgoren, N., and Lauritzen, M. (1998). Modification of activity-dependent increases of cerebral blood flow by excitatory synaptic activity and spikes in rat cerebellar cortex. *J. Physiol.* **512**, 555–566.
- Kayser, C., Kim, M., Ugurbil, K., Kim, D.S., and Konig, P. (2004). A comparison of hemodynamic and neural responses in cat visual cortex using complex stimuli. *Cereb. Cortex* **14**, 881–891.
- Lauritzen, M. (2005). Reading vascular changes in brain imaging: Is dendritic calcium the key? *Nat. Rev. Neurosci.* **6**, 77–85.
- Rees, G., Friston, K., and Koch, C. (2000). A direct quantitative relationship between the functional properties of human and macaque V5. *Nat. Neurosci.* **3**, 716–723.
- Heeger, D.J., Huk, A.C., Geisler, W.S., and Albrecht, D.G. (2000). Spikes versus BOLD: What does neuroimaging tell us about neuronal activity? *Nat. Neurosci.* **3**, 631–633.
- Hyder, F., Rothman, D.L., and Shulman, R.G. (2002). Total neuroenergetics support localized brain activity: Implications for the interpretation of fMRI. *Proc. Natl. Acad. Sci. USA* **99**, 10771–10776.
- Smith, A.J., Blumenfeld, H., Behar, K.L., Rothman, D.L., Shulman, R.G., and Hyder, F. (2002). Cerebral energetics and spiking frequency: The neurophysiological basis of fMRI. *Proc. Natl. Acad. Sci. USA* **99**, 10765–10770.
- Masamoto, K., Kim, T., Fukuda, M., Wang, P., and Kim, S.G. (2007). Relationship between neural, vascular, and BOLD Signals in isoflurane-anesthetized rat somatosensory cortex. *Cereb. Cortex* **17**, 942–950.
- Leopold, D.A., Murayama, Y., and Logothetis, N.K. (2003). Very slow activity fluctuations in monkey visual cortex: Implications for functional brain imaging. *Cereb. Cortex* **13**, 422–433.
- Hasenstaub, A., Shu, Y., Haider, B., Kraushaar, U., Duque, A., and McCormick, D.A. (2005). Inhibitory postsynaptic potentials carry synchronized frequency information in active cortical networks. *Neuron* **47**, 423–435.
- Abeles, M. (1982). Quantification, smoothing, and confidence limits for single-units' histograms. *J. Neurosci. Methods* **5**, 317–325.
- Hasson, U., Nir, Y., Levy, I., Fuhrmann, G., and Malach, R. (2004). Intersubject synchronization of cortical activity during natural vision. *Science* **303**, 1634–1640.
- Kreiman, G., Hung, C.P., Kraskov, A., Quiroga, R.Q., Poggio, T., and DiCarlo, J.J. (2006). Object selectivity of local field potentials and spikes in the macaque inferior temporal cortex. *Neuron* **49**, 433–445.
- Amir, Y., Harel, M., and Malach, R. (1993). Cortical hierarchy reflected in the organization of intrinsic connections in macaque monkey visual cortex. *J. Comp. Neurol.* **334**, 19–46.
- Hackett, T.A., Stepniewska, I., and Kaas, J.H. (1998). Subdivisions of auditory cortex and ipsilateral cortical connections of the parabelt auditory cortex in macaque monkeys. *J. Comp. Neurol.* **394**, 475–495.
- Engel, A.K., Fries, P., and Singer, W. (2001). Dynamic predictions: Oscillations and synchrony in top-down processing. *Nat. Rev. Neurosci.* **2**, 704–716.
- Singer, W., and Gray, C.M. (1995). Visual feature integration and the temporal correlation hypothesis. *Annu. Rev. Neurosci.* **18**, 555–586.
- Eckhorn, R., Bauer, R., Jordan, W., Brosh, M., Kruse, W., Munk, M., and Reitboeck, H.J. (1988). Coherent oscillations: A mechanism of feature linking in the visual cortex? *Biol. Cybern.* **60**, 121–130.
- Gray, C.M., König, P., Engel, A.K., and Singer, W. (1989). Oscillatory responses in cat visual cortex exhibit inter-columnar synchronization which reflects global stimulus properties. *Nature* **338**, 334–337.
- Munk, M.H., Roelfsema, P.R., Konig, P., Engel, A.K., and Singer, W. (1996). Role of reticular activation in the modulation of intracortical synchronization. *Science* **272**, 271–274.
- Womelsdorf, T., Fries, P., Mitra, P.P., and Desimone, R. (2006). Gamma-band synchronization in visual cortex predicts speed of change detection. *Nature* **439**, 733–736.
- Steinmetz, P.N., Roy, A., Fitzgerald, P.J., Hsiao, S.S., Johnson, K.O., and Niebur, E. (2000). Attention modulates synchronized neuronal firing in primate somatosensory cortex. *Nature* **404**, 187–190.
- Tiesinga, P.H., Fellous, J.M., Salinas, E., Jose, J.V., and Sejnowski, T.J. (2004). Inhibitory synchrony as a mechanism for attentional gain modulation. *J. Physiol. (Paris)* **98**, 296–314.

35. Juergens, E., Guettler, A., and Eckhorn, R. (1999). Visual stimulation elicits locked and induced gamma oscillations in monkey intracortical- and EEG-potentials, but not in human EEG. *Exp. Brain Res.* 129, 247–259.
36. Kayser, C., Salazar, R.F., and Konig, P. (2003). Responses to natural scenes in cat V1. *J. Neurophysiol.* 90, 1910–1920.
37. Eggermont, J.J., and Smith, G.M. (1995). Separating local from global effects in neural pair correlograms. *Neuroreport* 6, 2121–2124.
38. Nicholson, C. (1973). Theoretical analysis of field potentials in anisotropic ensembles of neuronal elements. *IEEE Trans. Biomed. Eng.* 20, 278–288.
39. Attwell, D., and Laughlin, S.B. (2001). An energy budget for signaling in the grey matter of the brain. *J. Cereb. Blood Flow Metab.* 21, 1133–1145.
40. Traub, R.D., Whittington, M.A., Stanford, I.M., and Jefferys, J.G. (1996). A mechanism for generation of long-range synchronous fast oscillations in the cortex. *Nature* 383, 621–624.
41. Privman, E., Nir, Y., Kramer, U., Kipervasser, S., Andelman, F., Neufeld, M.Y., Mukamel, R., Yeshurun, Y., Fried, I., and Malach, R. (2007). Enhanced category tuning revealed by intracranial electroencephalograms in high-order human visual areas. *J. Neurosci.* 27, 6234–6242.
42. Schneidman, E., Berry, M.J., 2nd, Segev, R., and Bialek, W. (2006). Weak pairwise correlations imply strongly correlated network states in a neural population. *Nature* 440, 1007–1012.
43. Olshausen, B.A., and Field, D.J. (2004). Sparse coding of sensory inputs. *Curr. Opin. Neurobiol.* 14, 481–487.